Design of a Single-Element Dynamic Antenna for Secure Wireless Applications

Amer Abu Arisheh, *Graduate Student Member, IEEE*, Jason M. Merlo, *Graduate Student Member, IEEE*, and Jeffrey A. Nanzer, *Senior Member, IEEE*

***Abstract*—We introduce a new technique for secure wireless applications using a single dynamic antenna. The dynamic antenna supports a constantly and rapidly changing current distribution that generates a radiation pattern that is static in a desired direction and dynamic elsewhere. This imparts additional modulation on the signal and obscures information transmitted or received outside of the information beam, thus achieving directional modulation. Dynamic currents are supported by a single feed that is switched between separate ports on a single antenna, generating two different radiation patterns without changing the physical shape of the antenna. We introduce the theoretical concept by exploring an ideal complex dynamic radiation pattern that remains static in a narrow desired direction and is dynamic elsewhere. The impact on the transmission of information is analyzed, showing that the information beam narrows as the modulation order increases, and design constraints on the spatial width of the information beam as a function of modulation format are determined. We design and analyze a 2.3 GHz two-state dynamic dipole antenna and experimentally demonstrate secure wireless transmission. We demonstrate the ability to change the information beamwidth and steer the information beam experimentally in real time, and to maintain high throughput in the information beam while obscuring the information elsewhere. In contrast to multiport or array-based antennas, our approach introduces a novel rapidly switched single-element technique for secure wireless applications that can be used independently from the rest of the wireless system, essentially operating as a "black box" for an additional layer of security.**

***Index Terms*—Directional modulation, dynamic antenna, fast switching, physical layer security, secure wireless communications, switched antenna**

I. Introduction

Security is rapidly becoming a central aspect of wireless system design. With the increase in wireless communications devices as well as wireless sensing systems, all of which are becoming increasingly connected via wireless networks, the potential for vulnerabilities, both from inadvertent and malicious means, is commensurately increasing. Vulnerabilities in wireless networks are an active area of research [1], however research on the security of emerging sensor systems such as automotive radar have also demonstrated the potential physical layer vulnerabilities of such systems [2], [3]. While security approaches for wireless systems have traditionally focused on digital security, there is significant interest in and potential for embedding security into the physical layer of wireless systems to serve as a first line of defense against unintended or malicious actions. Security at the physical layer reduces the burden on digital security protocols, thereby supporting better efficiency and throughput, and can potentially be implemented as a black box protocol that is transparent to the rest of the wireless system.

Various physical layer approaches to wireless security have been explored (see, e.g., [4]), including radio-frequency (RF) fingerprinting, signal coding, and multiple-input multiple-output (MIMO) architectures. However, the approaches that are closest to the physical wireless transmission and have the potential for little to no coordination with the rest of the system use the antenna system itself. Directional antennas or antenna arrays steer higher gain signal towards intended directions, with lower gain elsewhere, leading to reduced detectability and information recovery outside the mainbeam [5]. The antenna pattern is generally static and thus the same signal is broadcast to all directions; therefore, an eavesdropper that is close to the antenna or has a more sensitive receiver can still potentially recover the information. Dynamic antenna patterns have been implemented in array antennas to overcome this problem, creating a directional modulation on the transmitted (or received) signal at angles outside the mainbeam, thereby obfuscating the information and making it more difficult if not impossible to demodulate [6]–[9]. Such arrays have been implemented by controlling the excitation weights of each array antenna element [10], by reconfiguring the antenna radiating elements [11], or by using dynamic motion in distributed antenna arrays [12]. But while these approaches are feasible for array applications, many wireless systems use compact antennas, often single-elements, in which physical layer security is more difficult to impart. Some works have investigated the use of multiple antenna elements constructed within a compact space (e.g., [13], [14]), however these nonetheless require multiple signal feeds in order to impart directional modulation, increasing the complexity of the wireless system and preventing the physical layer approach from being transparent to the rest of the system.

In this paper, we present a new approach to physical layer wireless security based on a novel dynamic single-element antenna. Through random switching of the current path on the antenna structure, the current distribution on the element is dynamically modified, generating a dynamic radiation pattern that remains static in a desired direction and imparts additional amplitude and phase modulation in

This material is based in part upon work supported by the National Science Foundation under grant #2028736. *(Corresponding author: Jeffrey A. Nanzer)*

The authors are with the Department of Electrical and Computer Engineering, Michigan State University, East Lansing, MI 48824 USA (email: {abuarish, merlojas, nanzer}@msu.edu).

directions away from the information beam[1]. In contrast to reconfigurable antennas, which typically cycle through various states to find a desired radiation pattern, our dynamic antenna design is characterized by constant and rapid change in the radiation pattern, thereby creating additional time-varying modulation on the signal outside the information beam. The approach is simple and requires no computational analysis of the antenna states, similar to other synthesis-free directional modulation approaches [15]–[17]. We introduced the basics of the concept in [18], [19]; here we provide extensive detail on the underlying theory behind dynamic antennas and their use in directional modulation for various modulation formats and describe the ability to steer the information beam. We describe in detail the impact of dynamic amplitude and phase patterns. We present the design and the first experimental implementation of a 2.3 GHz dynamic dipole antenna, and experimentally demonstrate the use of the dynamic antenna for secure transmission of data in a wireless communications system. Our experiments show the ability to retain high throughput in the desired direction while mitigating throughput outside the information beam using dynamics at the same speed as the data. However, the presented approach need not dynamically switch at the same speed as the information, as lower or higher rates could be used if the application allows. Importantly, this means that the dynamic antenna system can operate effectively independent of the underlying wireless system, such that it can be used as an external add-on to existing wireless systems. Furthermore, while we show the use of communications systems, the approach also applies to secure wireless sensing (on both transmit and receive).

The information conveyed in a secure wireless system can be implemented at various points in the system, and directional modulation may be imparted through various approaches. Techniques such as array-based reconfigurable element weighting [6], [8], [10] and direct antenna modulation [7], [11] impart modulation of the information on the transmitted or received signals directly at the radiating elements, effectively synthesizing the information at the aperture. These approaches necessitate a close tie between the wireless system and the aperture itself such that the full system must be co-designed. Other approaches have implemented directional modulation via multiport structures composed of collocated elements and leverage the addition of complex noise for directional modulation [14], [20], [21]; however, this reduces power efficiency [14] and necessitates multiple simultaneous signal feeds. For these types of structures, steering of the information beam generally requires a characterization of all states of the antenna structure to essentially generate a look-up table of states mapping to steering angles. Synthesizing such information can not only be time-consuming and subject to errors, but may also need to be done for each antenna due to manufacturing variations that impact the directional modulation quality. In contrast to the above approaches, our system imparts additional modulation onto the transmitted or received signals using a single antenna. The baseband digital information is synthesized normally using a traditional communications system to which the dynamic antenna is connected. Aside from knowing the information rate, the aperture can effectively be decoupled from the communications system, acting as a "black box" that adds an additional layer of security without otherwise impacting the communications system. Also, our approach uses only a single signal port, which is rapidly switched between two locations on the antenna structure. This allows for the antenna to be implemented in place of existing antennas on legacy systems as well as integrated into future wireless systems. Furthermore, steering of the information beam is easily implemented using simple relative weighting of the complex signals between the feed points on the antenna, rather than a rigorous antenna state characterization. Overall, our antenna design provides a simple, flexible approach to adding directional modulation onto wireless systems for added security. The novel contributions of this work are as follows.

- We present a new approach to achieving radiation pattern dynamics in single antenna systems that is characterized by constant change in the antenna current distribution at a rate commensurate with the rate of information transmitted or received by the antenna.
- We present the first design and demonstration of a single-antenna approach to directional modulation.
- Information beam steering is demonstrated using simple relative weighting of the signals between the feed points on the antenna.
- Our approach is based on the characterization of information, yielding a system-focused approach that naturally lends itself to the co-design of the electromagnetic components and communications system, and that may be adapted for use in existing legacy systems.
- We experimentally demonstrate real-time secure wireless communications using a straightforward test setup that can be easily replicated for other secure wireless research efforts.

The rest of this paper is outlined as follows. In Section II we present the foundational concept in detail, describing the effects of an ideal dynamic radiation pattern on information throughput as a function of angle. A numerical assessment is provided in Section III. In Section IV, a $3\lambda/2$ printed dipole antenna is designed based on the theoretical concepts from Section II. In Section V, the dynamic antenna is fabricated and measured, and Section VI-B presents comprehensive measurements of the antenna in a wireless communication system. In Section VI-D, we demonstrate how the information beam can be steered. Finally, Section VII concludes this work.

II. Directional Modulation Using a Single Dynamic Antenna

The radiated fields of any antenna are governed by the current flowing in that antenna. Thus, in general, feeding an antenna from two different feed points yields different radiation patterns versus angle. We start abstractly without confining ourselves to any particular antenna and consider a general single-port two-state switched antenna in Fig. 1, which shows the two feed points colored in red and blue. This

[1]We define the *information beam* as the beamwidth over which the information is recoverable, e.g. [7].

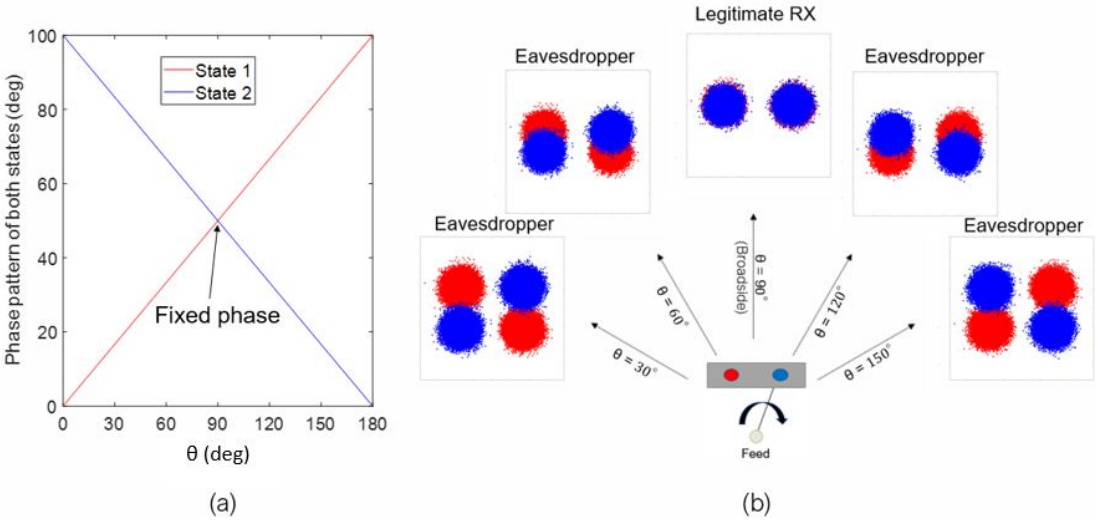

Fig. 1. Phase dynamics of a hypothesized antenna for directional modulation. (a) Phase patterns generated by a notional antenna by connecting the feeding port to the red feed point (State 1) and by connecting the feeding port to the blue feed point (State 2); isotropic amplitude patterns are assumed. (b) Constellations obtained by modulating a pseudo random bit sequence (PRBS) by the phase patterns with 12 dB SNR. The signals are standard in the direction of the legitimate receiver, but distorted elsewhere.

antenna has a single feeding port and a switch that connects it to either the red or blue feed point, creating two states of the antenna. Fig. 1(a) shows notional phase patterns radiated when feeding the antenna through the red or blue feed point, respectively. We assume the amplitude to be static versus angle for both states. While the physical realizability of such an antenna is not considered, the theoretical radiation pattern serves as a construct to demonstrate the impact of dynamic phase patterns. Fig. 1(b) shows the scatter diagram (constellation) of a demodulated binary phase shift keyed signal received by the two states at various angles. The constellations are obtained by modulating a pseudo random bit sequence (PRBS) by the phase pattern shown in Fig. 1 while assuming isotropic amplitude pattern with 12 dB SNR. While switching may be implemented randomly, throughout this paper we assume uniform switching. It is assumed that the legitimate receiver is in the broadside direction while eavesdroppers exist elsewhere. The received constellation at the broadside $\theta = 90^{\circ}$ is the standard binary phase shift keying (BPSK) diagram and is equal for both states since the phase pattern is equal at broadside. This implies that the legitimate receiver will not be affected by switching between the two states of the antenna. However, away from broadside the phase patterns of the two states impart additional phases, yielding rotation between the two constellations. This implies that the eavesdroppers will receive non-standard constellations. For example, at $\theta = 30^{\circ}$, we notice that the eavesdropper is receiving a constellation that looks similar to a quadrature-phase shift keyed (QPSK) signal. The impact of the phase rotation on the data is dependent on the modulation format. Increasing the transmitted modulation order to 4-level quadrature amplitude modulation (4-QAM) as shown in Fig. 2 or 64-QAM as shown in Fig. 3, the constellations away from broadside are more affected by the phase dynamics since there is less phase difference between adjacent symbols. Since the eavesdropper sees the

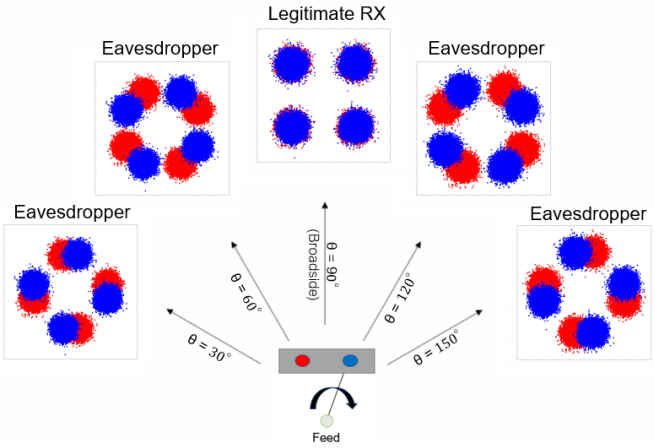

Fig. 2. Phase dynamics of a hypothesized antenna achieving directional modulation for 4-QAM.

constellation diagram as the aggregate of the diagrams of the two states, it may be difficult or impossible to demodulate the underlying data. Furthermore, at some angles, the phase rotation may be such that separate symbols in each state land on the same point in the constellation (see Fig. 4), making demodulation more difficult.

Information beam steering can be accomplished directly by weighting (in amplitude or phase) the signal prior to the feedpoint(s). The fact that each of the two states corresponds to separate complex radiation patterns allows for a simple calibration, and does not require a rigorous analysis of all antenna states (e.g, [17]). For example, to steer the information beam in Fig. 1 to $\theta = 120^{\circ}$, a phase shift to state 2 equal to the difference between the two states at $\theta = 120^{\circ}$ which equals 33.33° is added, producing static fields in that desired direction as shown in Fig 5.

While the above analysis focused on phase dynamics,

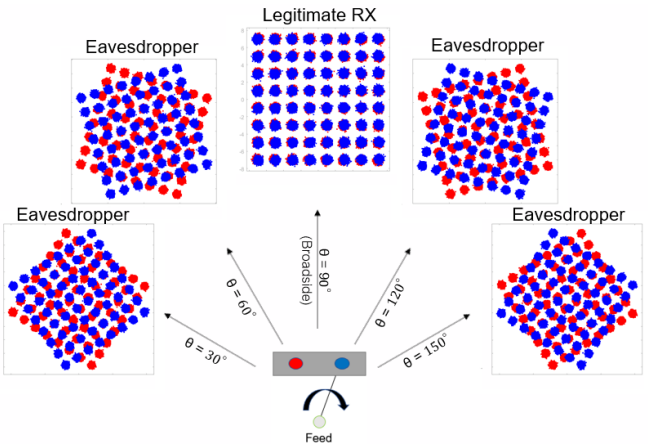

Fig. 3. Phase dynamics of a hypothesized antenna achieving directional modulation for 64-QAM.

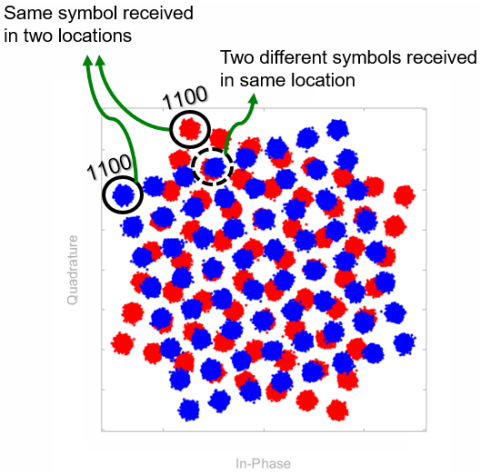

Fig. 4. Constellation at $\theta = 60$ (Fig. 3). Phase dynamics distort the constellation of symbols via rotation. The summation is clearly distorted by shifting symbols to different locations, but also sometimes with different symbols received in the same location.

similar results can be obtained with amplitude dynamics. The previous discussion of phase dynamics assumed an isotropic amplitude pattern. We now analyze the complementary problem by assuming that the radiated fields exhibit isotropic phase patterns, while amplitude patterns are assumed to be as shown in Fig. 6(a). (Similar to the phase pattern analysis, we consider this theoretical radiation pattern as a construct to demonstrate the impact of dynamic amplitude patterns.) Consequently, Fig. 6(b) shows the received constellations with 12 dB SNR at the broadside direction and 16-QAM modulation. The constellation in the broadside is standard due to the fixed amplitude, while away from broadside the constellation is distorted due to the amplitude difference between the two states.

This constellation interpretation of directional modulation is intuitive and can be expanded in different directions. For example, while some other works configure systems for a specific digital modulation scheme, this technique works directly for any QPSK or QAM modulation order [6]–[8], [10]. Also, standard constellations can be obtained in our technique by making a perfect amplitude and phase calibration, in contrast to some other techniques. Moreover, the antenna can operate normally without exhibiting dynamics by simply fixing the antenna to operate to only one of the states. Furthermore, it can be easily converted to be more challenging to the eavesdropper by increasing number of feedpoints, which increases number of states (and constellations), which makes it more challenging for the eavesdropper. It can also be used to achieve dynamic directional modulation [9]; however, this paper demonstrates the fundamental case of only two states.

We conclude this theoretical section by summarizing the design requirements. To support directional modulation, the dynamic antenna should support a static complex radiation field at the legitimate RX direction(s) and sufficiently dynamic amplitude and/or phase patterns elsewhere. In essence, the patterns A_i and A_j of antenna states i and j should be appreciably different outside the desired steering direction θ_0 in amplitude and/or phase while being equal at θ_0, i.e.,

$$||A_i(\theta)| - |A_j(\theta)|| \begin{cases} \geq \alpha, & \theta \neq \theta_0 \\ = 0, & \theta = \theta_0 \end{cases} \quad (1)$$

and/or

$$|\angle A_i(\theta) - \angle A_j(\theta)| \begin{cases} \geq \beta, & \theta \neq \theta_0 \\ = 0, & \theta = \theta_0 \end{cases} \quad (2)$$

where α and β are thresholds determined by parameters such as the modulation format. This should hold over the bandwidth of the information; if passband variations exist additional analysis may be necessary to evaluate the resultant modulation. Note that the pattern symmetry between the two states shown in Fig. 1 is not strictly necessary. Information beam steering may result in some loss of power at places that have differences in the amplitude pattern, thus the design should minimize this loss at the desired directions. The aforementioned complex radiation pattern requirements can be met with various antenna types such as beam steering antennas, reconfigurable antennas and pattern reconfigurable antennas. However, the kind of switches and control circuitry might need to be modified to match the switching requirements.

III. Simulation of Information Transfer with a Dynamic Antenna

In this section, we perform a numerical assessment in MATLAB to assess our theoretical technique for directional modulation introduced in Section II. We analyze through simulation the bit-error ratio (BER) obtained as a function of angle for both phase and amplitude dynamics. We simulated PRBS signals with Gray coding and calculated the BER as a function of angle with the effect of the dynamic antenna patterns included. Standard forward error correction (FEC) codes can reliably recover information when BER $< 10^{-3}$, thus it is desired that the BER in the information beam be below this threshold, while outside the information beam it should be greater. Fig. 7(a) and Fig. 8(a) show the resultant BER for noise-free channels for different modulation rates using phase dynamics and amplitude dynamics, respectively. We assume the worst case where the eavesdropper knows the modulation order and the bit rate. It can be seen that an information beam

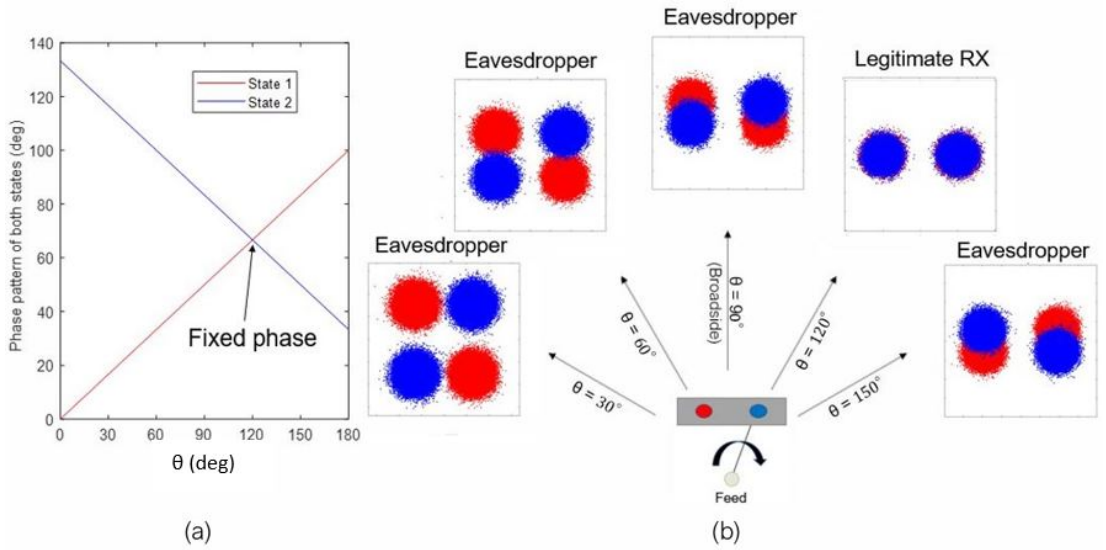

Fig. 5. Phase dynamics of the antenna after steering information beam to $\theta = 120°$. (a) Phase patterns generated by adding a constant phase shift to port 2 (State 2) which equals the difference between the two phase patterns at $\theta = 120°$; consequently, this yields a static phase at that angle. (b) Constellations obtained by modulating a PRBS by the phase patterns with 12 dB SNR.

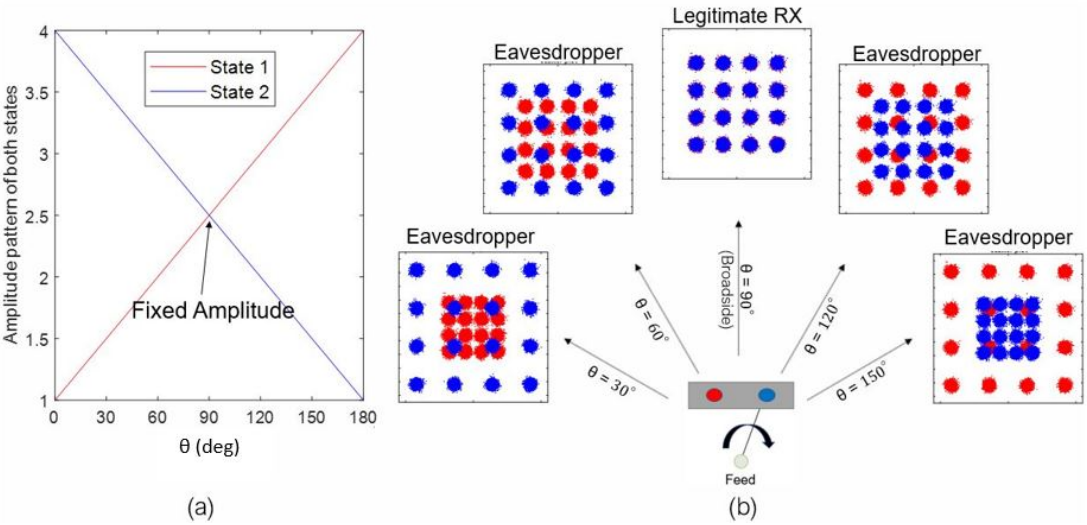

Fig. 6. Amplitude dynamics of a hypothesized antenna for directional modulation. (a) Amplitude patterns generated by a notional antenna by connecting the feeding port to the red feed point (State 1) and by connecting the feeding port to the blue feed point (State 2); isotropic phase patterns are assumed. (b) Constellations obtained by modulating a PRBS by the amplitude patterns with 12 dB SNR.

is obtained for each modulation format (centered at 90°) and that higher order modulation formats incur more errors away from the information beam, as expected due to the decreased separation between the symbols. Note that since there is no noise, the increase in BER outside the information beam is due solely to the modulation imparted by the antenna element dynamics. Furthermore, the addition of noise will thus serve to narrow the information beam further.

Figs. 7(b) and 8(b) show the difference between the two states in the phase dynamics and amplitude dynamics cases, respectively, in addition to a threshold line for each modulation scheme below which zero BER is obtained. In other words, these threshold lines indicate the minimum amount of difference in phase or amplitude required to cause an error. These threshold lines show how the information beamwidth can be altered by changing the modulation order. Note that the information beamwidth can be mathematically calculated without complicated simulations. For example, in the phase dynamics case, for PSK modulation orders, the threshold can be determined by simply noting that this line marks the angle at which an overlap starts to occur between different symbols; thus we obtain the threshold value for each case by dividing 360° by the corresponding PSK modulation order.

IV. Switched Dipole Antenna Design

The above analysis shows the impact on wireless transmission from amplitude or phase dynamics separately; in practice, the amplitude and phase patterns of an antenna are

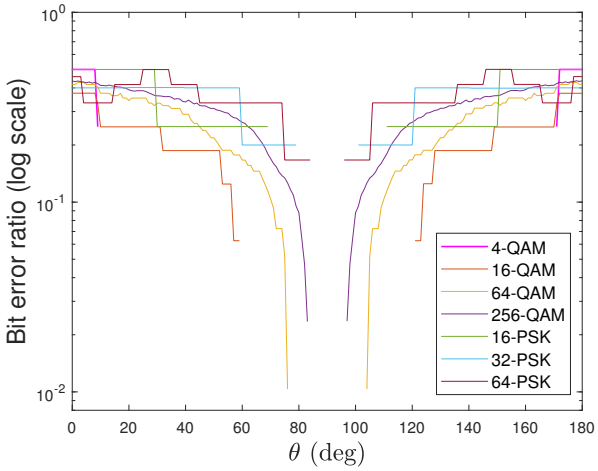

(a)

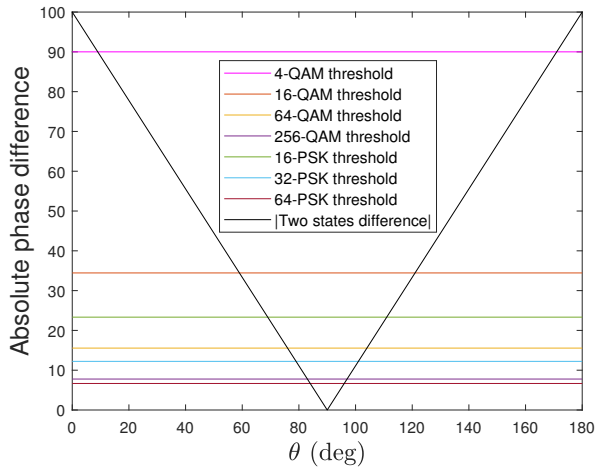

(b)

Fig. 7. Bit error ratio using phase dynamics with no amplitude dynamics and a noise-free channel. The receiver is assumed to know the bit rate and modulation format. (a) BER versus angle for various QAM and PSK orders showing that larger orders are more affected and yield a narrower information beam. (b) The difference between the two phase patterns with thresholds lines below which the corresponding modulation schemes exhibit low BER.

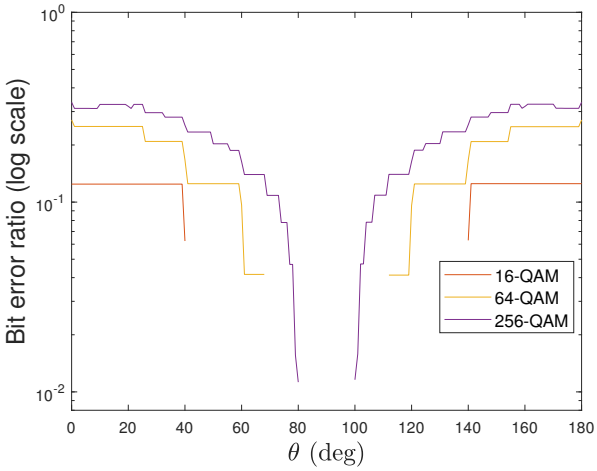

(a)

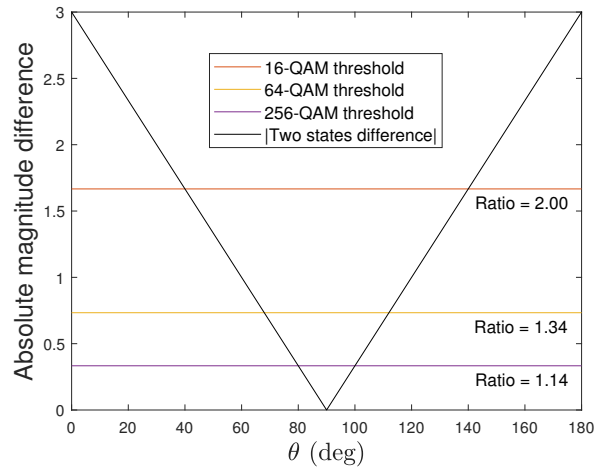

(b)

Fig. 8. Bit error ratio using amplitude dynamics with no phase dynamics and a noise-free channel. The receiver is assumed to know the bit rate and modulation format. (a) BER versus angle for various QAM orders showing that larger orders are more affected and yield a narrower information beam. (b) The difference between the two amplitude patterns with thresholds lines below which the modulation schemes exhibit low BER. For each threshold line, the ratio of the two amplitudes is also shown, to indicate the relative differences between the amplitude values.

coupled, thus the goal is to obtain a pattern that is static in both phase and amplitude in the broadside direction when switched between two states, and that exhibits dynamics in phase and/or amplitude at angles away from broadside. Our design is based on an asymmetrically-fed 2.26 GHz $3\lambda/2$ dipole antenna whose input signal is switched between two symmetric points on the antenna at distance of $\pm\lambda/2$ with respect to the center (see Fig. 9). For any dipole antenna, by switching between two ports having same distance from the center, and shorting the current path on the unused port, the current distribution is mirrored between the two antenna states; in theory, the antenna pattern will thus remain static at broadside and will change at angles away from broadside. The $3\lambda/2$ dipole was chosen specifically because it is a classical case that exhibits a mainbeam along with only two sidelobes. By feeding the dipole at an off-center location, the radiation at the two sidelobes will be asymmetric. Thus, by feeding the antenna at two off-center feedpoints, both the same distance from the center of the antenna, and switching between them, dynamics in the sidelobes manifest, while the phase and amplitude of the mainbeam remains relatively constant. On the other hand, the half-wavelength dipole can be well-matched only at or close to the center of the antenna, whereas the $3\lambda/2$ dipole can be well-matched at off-center locations also which satisfy our requirement for asymmetric radiation pattern.

Fig. 10 shows the radiation patterns of the two states; since the feed points of the two states are symmetric, generating mirrored current densities, the resultant radiation patterns are likewise mirrored. Since the antenna is long compared to a wavelength, multiple lobes manifest. The lobe at broadside is constant between the two states, while the two adjacent

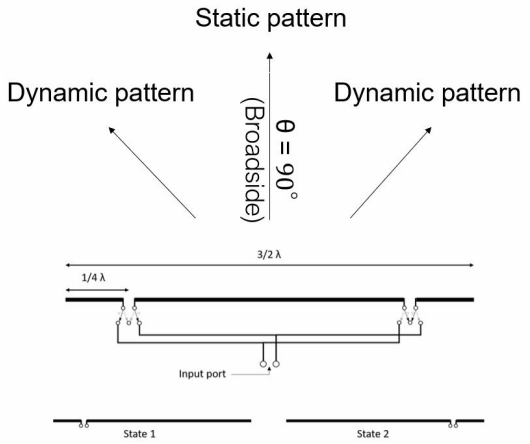

Fig. 9. The basic concept of dynamic pattern $3\lambda/2$ dipole antenna. The antenna switches between two states that mirror each other; with each state generating an asymmetric radiation pattern. Thus, the pattern in the mainlobe is static while it is dynamic elsewhere.

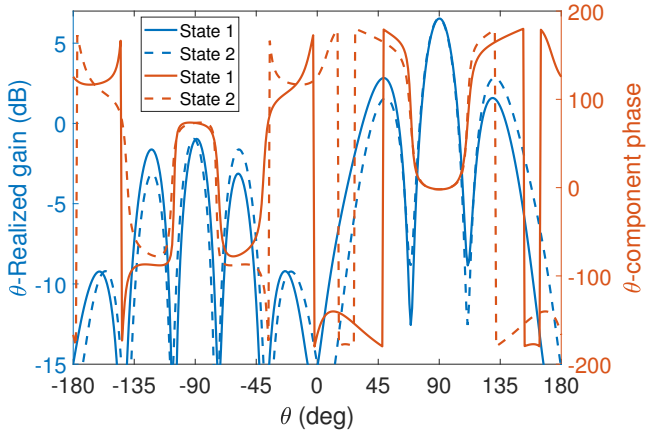

Fig. 12. Amplitude pattern and phase pattern of the simulated static printed dipole at 2.26 GHz. The central forward region has a quasi-static fields in addition to other three regions in the backside.

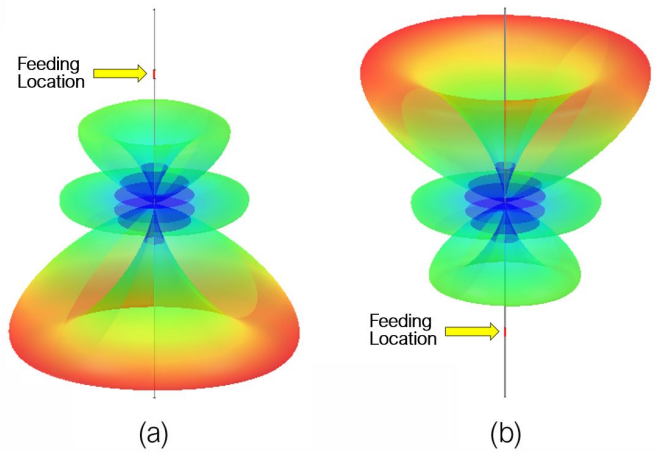

Fig. 10. (a) Radiation pattern (linear scale) of a $3\lambda/2$ dipole antenna fed at $+\lambda/2$ and (b) fed at $-\lambda/2$ with respect to the center.

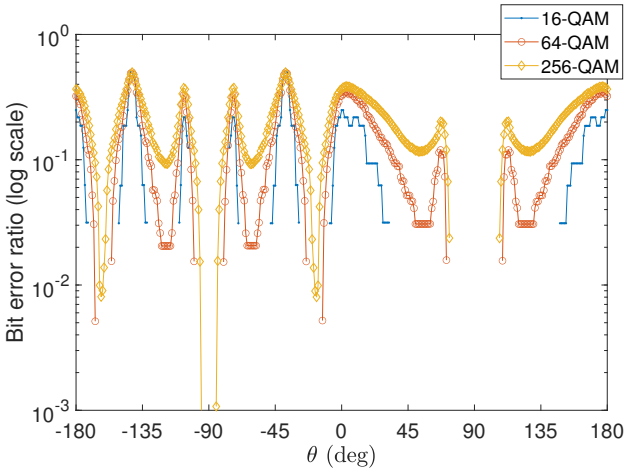

Fig. 13. BER in a noise-free channel using the amplitude pattern and phase pattern shown in Fig. 12.

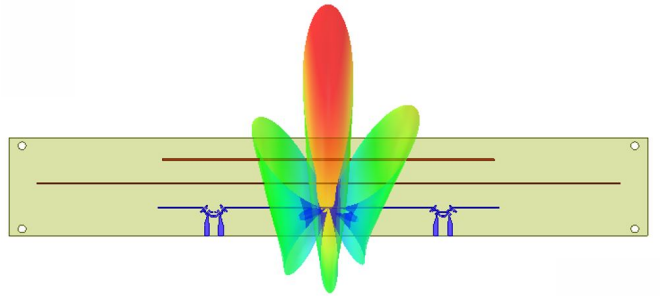

Fig. 11. Printed dipole design with two parasitic elements and its radiation pattern plotted at 2.26 GHz (linear scale) when fed on the left port. The central lobe is the largest and radiation is mainly in the forward direction, broadside to the dipole, with amplitude variation remaining on the sidelobes.

sidelobes exhibit large differential amplitudes. Such an antenna could feasibly be used for single-element directional modulation, however with reduced gain in the mainbeam.

To overcome the reduced gain in the broadside beam, two parasitic directive elements were added, and the antenna was designed to be printed on a Rogers RO4350B dielectric substrate with thickness of 1.524mm, as shown in Fig. 11. The antenna uses a balanced feed with coplanar striplines [22], [23]. While our design is based on a classical $3\lambda/2$ dipole antenna, we note that other designs can yield good directivity and sidelobe levels in a compact size (e.g. [24], [25]). The length of the dipole radiator is 148.08 mm, the longer parasitic element is 253.33 mm, and the shorter parasitic element is 144.08 mm. The width of each line is 0.55 mm and the distance between the center of any two consecutive elements is 10.37 mm. The feeding lines have a length of 4.5 mm (before tapering), a width of 2 mm, and their centers are separated by 6.19mm. The length and width of the substrate are 277.08 mm and 42.83 mm.

The radiation pattern overlaid on the antenna is the result of feeding the left port. The realized gain and phase patterns for both states is plotted in Fig. 12. The addition of the directors has a significant impact on the center lobe and sidelobes, as most of the signal energy is now constrained to the center lobe with a large front-to-back ratio (FBR). However, there remains an amplitude imbalance between the two sidelobes;

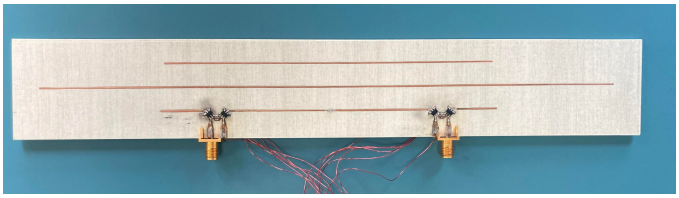

Fig. 14. Fabricated switched dipole antenna using four switches. The wires are used to control the switches by a microcontroller (MCU). Either one of the two feeding lines carry the signal at a time with an external switch changing the signal feed between them. This external switch is also controlled by the MCU to form either State 1 or State 2.

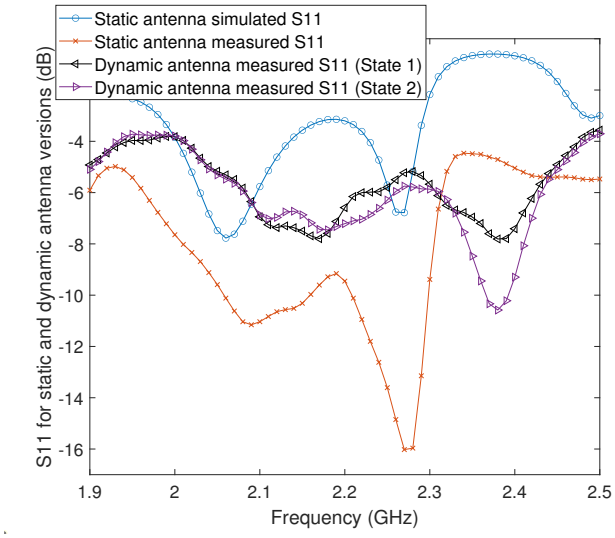

Fig. 15. S11 of simulated static antenna, printed static antenna, and the dynamic printed dipole.

this is necessary to ensure that the radiation pattern in the sidelobes is dynamic when switching between the two states, as the radiation pattern will be mirrored for the other state.

We simulated the BER in a noise-free channel, assuming the eavesdropper knows the bit rate and modulation order, using the amplitude and phase patterns from the simulated antenna. The corresponding BER curves are shown in Fig. 13. Note that there are quasi-static fields in the central forward lobe, and also in three directions in the backward region. Note that information beam in the forward direction is not greatly reduced when moving from 64-QAM to 256-QAM because there is no appreciable amplitude or phase dynamics in this region as shown in Fig. 12. Note also that we have three other information beams in the backward central direction; however, the realized gain there is small, thus the addition of noise in the simulation will remove these areas of low BER.

V. Dynamic Antenna Fabrication and Measurement

A static version of the printed dipole in Fig. 11 was initially fabricated to evaluate the radiation pattern; the State 1 (left) feedport was connected to an SMA connector while the second feedport was shorted. This antenna resonated at 2.27 GHz, close to the simulated resonance frequency. The radiation pattern was measured at 2.275GHz and exhibited

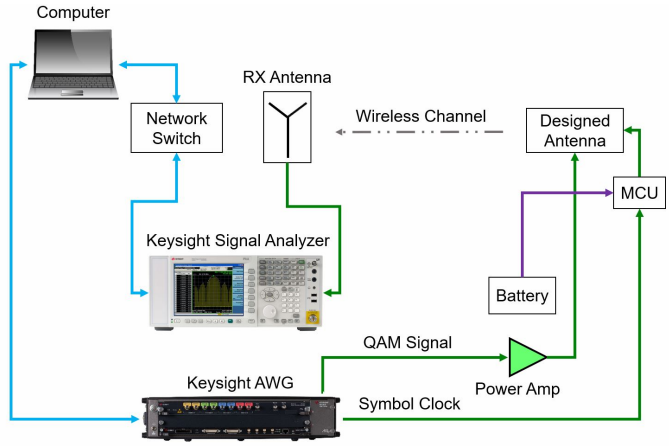

Fig. 16. Experimental communications system setup. The AWG transmitted data through an amplifier to the antenna which is switched synchronously with the symbol clock; the receiver (RX) send the signal to the signal analyzer.

a realized gain of approximately 1.5 dBi and a FBR of approximately 6 dB. The switched dynamic printed dipole was fabricated using 4 switches (HMC545AE) and 7 capacitors (0603ZA101JAT2A), and is shown in Fig. 14. There is one signal feeding port that feeds the antenna system through an external switch (HMC595A) which connects it to either port 1 feed line (to form State 1) or port 2 feed line (to form State 2). This external switch in addition to the four switches on the antenna are controlled by a microcontroller (MCU). The simulated and measured S11 of the single-state antenna and that of the two states of the dynamic antenna are shown in Fig. 15. The simulations were conducted in HFSS and did not include models of the switches on the antenna, instead replacing them with short circuits for the appropriate switch state, thereby adding some mismatch between the simulated and measured designs. Inclusion of the switches resulted in an increase in the resonance frequency from 2.26 GHz to 2.385 GHz, and furthermore imperfect matching between the switches and the antenna lines resulted in a worse match. Nonetheless, the two states are consistent, resonate at the same frequency, and approach –10 dB S11. Future work to improve the match between the switches and the antenna lines would serve to improve the S11.

However, the calculated gain for this dynamic printed antenna is around –4 dBi, which is due to the mismatch of the four switches existing in the current path. The switches are designed to be connected to 50 ohm feed lines above a ground; a future design will seek to optimize the impedance matching to the switches, which should lead to increased gain closer to that of the static design. Nevertheless, our design is sufficient to demonstrate the technique and show that it can work in short distance applications such as WiFi.

VI. Experimental Demonstration in a Wireless Communication System

A. System Design

The block diagram of the experimental system is shown in Fig. 16. A communications signal is generated directly at

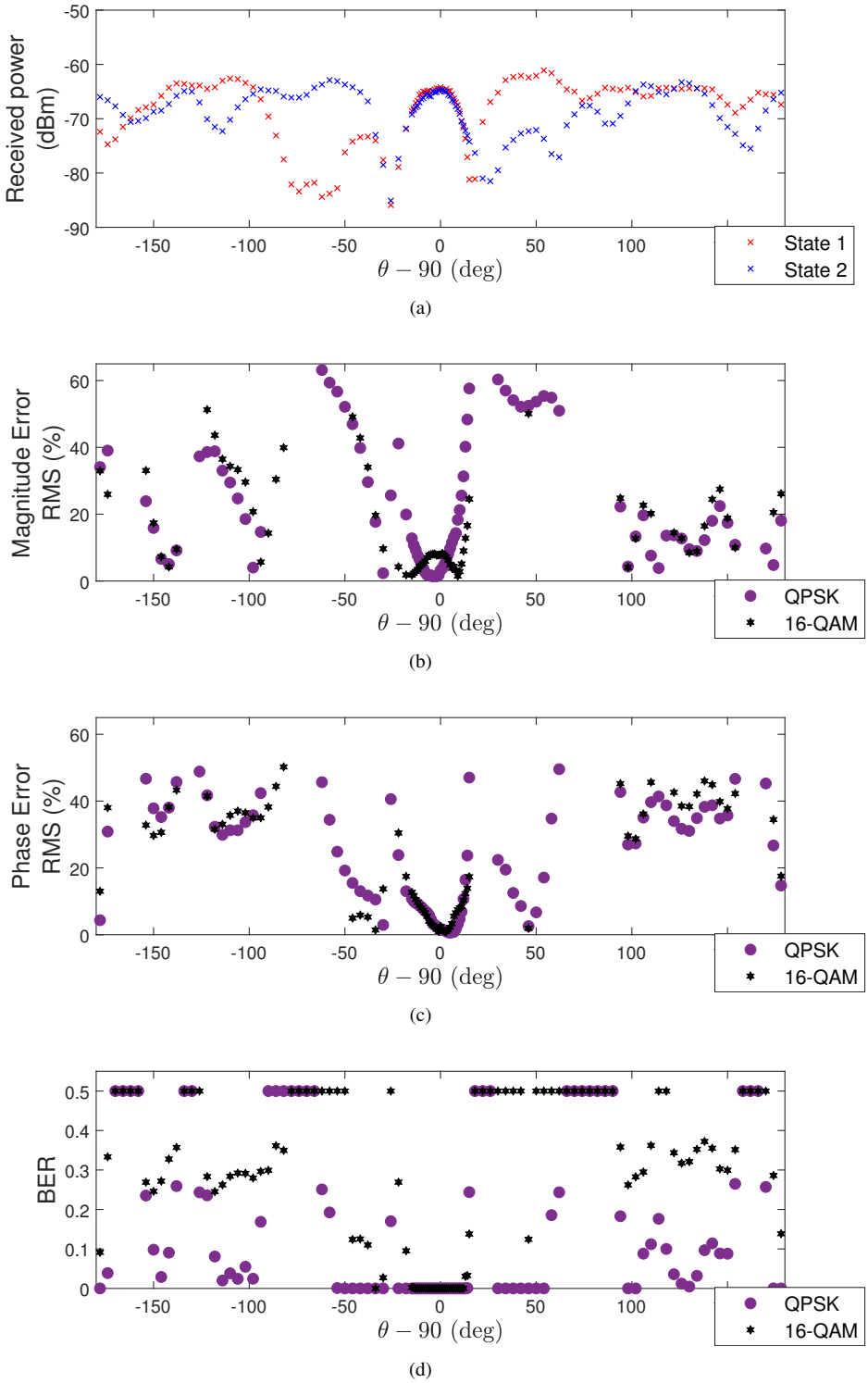

Fig. 17. Measured radiation patterns and error parameters of the dynamic switched antenna when transmitting QPSK or 16-QAM at 2.385 GHz with 1 MHz symbol rate. (a) Radiation patterns of the two static states. (b) Magnitude error during switching. (c) Phase error during switching. (d) BER during switching. The antenna was rotated in a one-degree step in the region from –15° to +15° to increase sampling in the information beam, while four-degree jumps were taken outside this region (–18° and above +18°). The magnitude error and phase error provide a measure for the radiation pattern distortion due to switching; they are related to the BER: large errors are obtained when either is large. The measurement setup and environment can be considered almost noise free since no errors appeared for the static measurements, even at the nulls and low power regions of the two static states radiation patterns. Some angles are left empty since the signal was so distorted that no data could be demodulated; at these angles, the BER was set to 0.5. Thus, all errors detected were due solely to dynamic switching of the antenna.

a 2.385 GHz carrier frequency using a Keysight M8190A Arbitrary Waveform Generator (AWG) then amplified and passed to the antenna under test. The antenna transmits the signal while it is dynamically switched between the two states by the MCU, synchronously with the symbol clock. The radiated signal is received by a HG2458-08LP-NF log periodic antenna and sampled in a Keysight N9030A PXA Signal Analyzer. The PC used Keysight IQtools and PathWave Vector Signal Analysis software to generate and demodulate the communications signals in real time.

The dynamic antenna was calibrated for quasi-static amplitude and phase among the two states at broadside. A phase shifter was connected to the cable going to port 1 to align the phases between the two states, and a 6-dB attenuator was connected to the cable going to port 2 to match the amplitudes of the two states. These imbalances were due largely to differences in the cables and losses in the switches and phase shifter; in an integrated design the imbalances would be less and also easier to correct with small changes in microstrip lengths, etc.

The antenna was measured in both a static and dynamic cases in a semi-enclosed anechoic environment at a center frequency of 2.385 GHz. The antenna was rotated in one-degree increments in the region from -15° to +15°, which is in the main beam, and in four-degree increments outside this region. The measured power from the two states of the antenna when driven statically (no switching) is shown in Fig. 17(a), which clearly shows the consistency of the main beam between the two states, and the difference in the sidelobe power between the two states. For measuring the BER as a function of angle, $2^{11}-1$ PRBS signals of length 30,000 symbols were transmitted from the dynamic antenna with QPSK and 16-QAM modulation formats at a symbol rate of 1 MSps. 48Kbits were used to compute the error metrics at each angle. Demodulation was performed assuming knowledge of the transmitter parameters such as modulation format and symbol rate, representing a worst-case eavesdropper.

B. Measured Results vs. Angle

The measured magnitude error, phase error, and BER versus angle are shown in Figs. 17(b), 17(c) and 17(d), respectively. The magnitude error is the RMS average of the difference in amplitude between the I/Q measured signal and the I/Q reference signal. The phase error is the phase difference between the I/Q reference signal and the I/Q measured signal, averaged over all symbol points. In these three plots, and for some of the angles where distorted signals appear, then there was nothing detected in the reception side which most likely indicates that the signal was distorted to the level that reception was not possible. These regions were left empty in Figs. 17(b) and 17(c) while they were replaced with the value 0.5 in the measured BER plot (Fig. 17(d)) as 0.5 is the worst case BER value. The magnitude error (Fig. 17(b)) is consistent with the differences in the received power between the two states as indicated in Fig. 17(a): very small error is seen near broadside, indicating that the dynamic switching has a negligible effect on the transmitted data, whereas at other angles the error is high due to the additional modulation imparted on the signal from dynamic switching. Similarly, the phase error (Fig. 17(c)) is small in the mainbeam and appreciable elsewhere. Note that although the phase error is low in the two sidelobes adjacent to the mainbeam, the magnitude error is high; since either amplitude or phase dynamics will impart directional modulation, the signal will be modulated in amplitude in the adjacent sidelobes. This is clearly shown in the measured BER (Fig. 17(d)). The QPSK case exhibits zero or very small BER ($< 10^{-3}$) at various angles that are not limited to the broadside direction. However, the 16-QAM case only reliably has BER $< 10^{-3}$ in the region from -12° to 13°. This demonstrates the theory described earlier that large modulation orders are more affected by magnitude and phase dynamics. Note that although the main beam in the fabricated antenna is not significantly larger than the sidelobes as we aimed for in the design stage, the BER is nonetheless high in the directions of the sidelobes, indicating that information is not transferred.

Measurements of static antenna states (State 1 or 2 without switching) were conducted by measuring the BER at the nulls and low power regions shown in Fig. 17(a), when transmitting 16-QAM signals. All of these regions yielded zero BER. A static antenna exhibits errors mainly in nulls and other low gain regions where the SNR is poor; thus, since the BER was zero in the static case even at the nulls, all errors generated in the dynamic case were the result of dynamic switching, and not low SNR. The measurements thus closely resembled the noise-free channel case assumed in the simulations above despite the antenna gain.

C. Received Data

Examples of constellation diagrams and eye diagrams captured at the receiving antenna are discussed here for the QPSK and 16-QAM cases to elaborate more on the relation between the three error metrics we just discussed, i.e., magnitude error, phase error, and BER. The samples for QPSK case are shown in Fig. 18 at angles 0°, 114°, and –178° with the corresponding measured BER. At broadside (0°) the magnitude error and phase error are small, and constellation and eye diagram look standard. At 114°, there is a small magnitude error and large phase error that resulted in a constellation with four major points, however the symbols here are misplaced as in Fig. 4, leading to a distorted eye diagram and high BER (0.176). Another interesting case is shown at angle –178° at which there is a large amplitude error and small phase error; however, PSK modulation orders are not affected by amplitude dynamics and thus the measured BER at this angle is zero.

Constellation diagrams and eye diagrams of similar scenarios for the QAM-16 case are provided in Fig. 19. The angles studied are 0°, –94°, and 46°. For the 0° angle then we have a standard QAM-16 signal. The –94° case has small magnitude error and large phase error leading to distorted diagrams and a BER of 0.296. In this case, magnitude and phase error relation is analogous to that of the QPSK case at 114°, shown in Fig. 18(b), since both QPSK and 16-QAM are affected mainly by phase dynamics at this angle. Another interesting case occurs at angle 46° which has a large magnitude error and

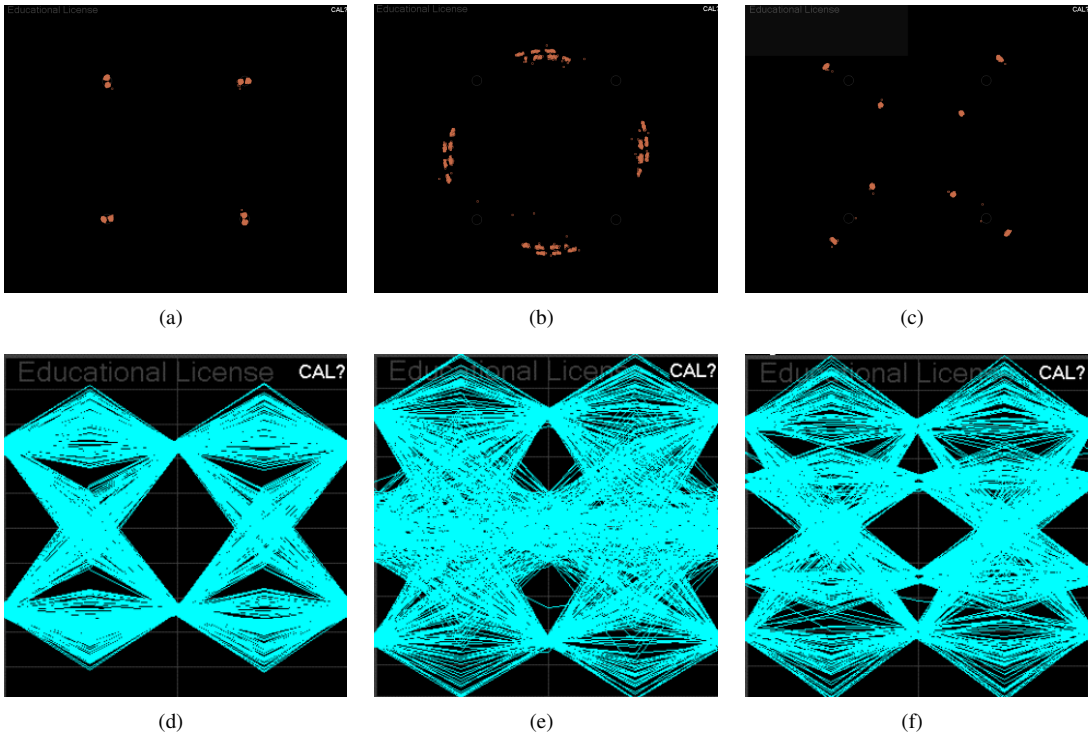

Fig. 18. Measured constellations and eye diagrams for QPSK signals at 0° [(a) and (d)], 114° [(b) and (e)], and –178° [(c) and (f)]. (a) and (d) correspond to BER = 0; (b) and (e) correspond to BER = 0.176; (c) and (f) correspond to BER = 0.

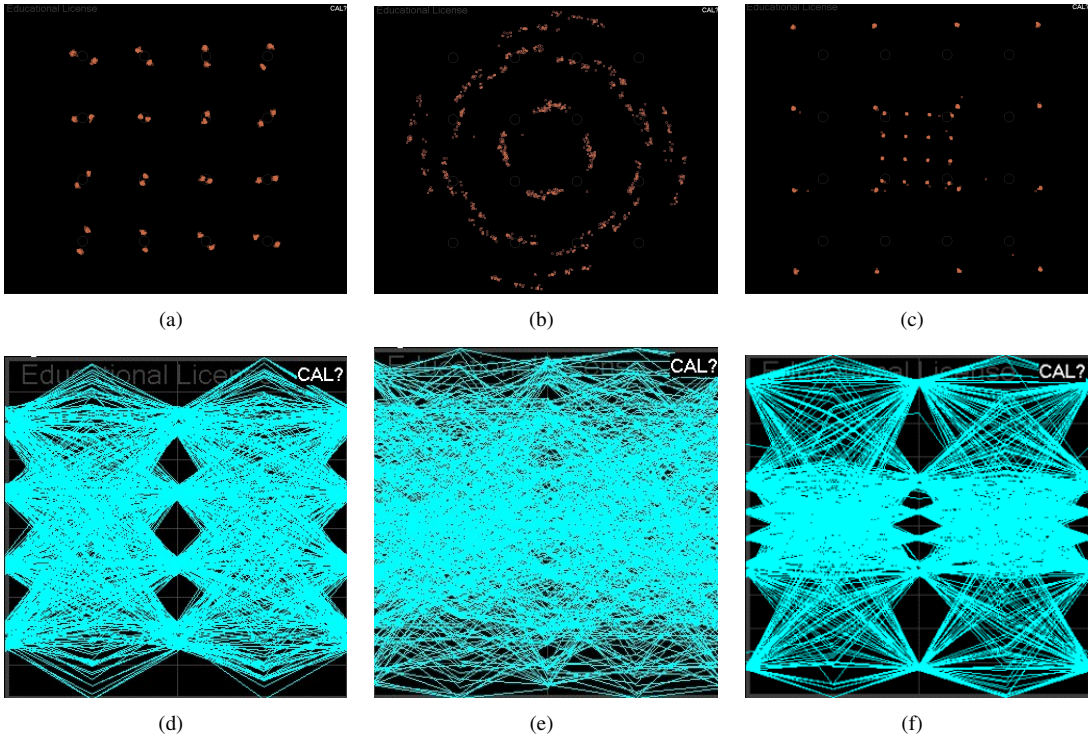

Fig. 19. Measured constellations and eye diagrams for 16-QAM signals at angles 0° [(a) and (d)], –94° [(b) and (e)], and 46° [(c) and (e)]. (a) and (d) correspond to BER = 0; (b) and (e) correspond to BER = 0.296; (c) and (f) correspond to BER = 0.124.

small phase error. As expected, this yielded large BER (0.124) since general large QAM modulation schemes are affected by amplitude dynamics.

D. Steering the Information Beam

As discussed in Section II, the information beam can be steered by correcting for the phase and amplitude imbalance between the two states at a desired angle. This can be obtained

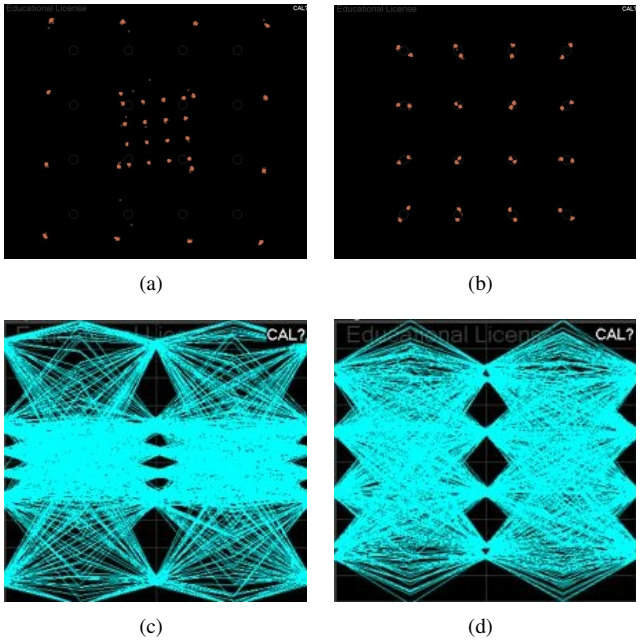

Fig. 20. Measured constellations and eye diagrams for 16-QAM signals where the information beam was steered to 46° at angles 0° [(a) and (c)] and 46° [(b) and (d)], showing a clear constellation at the beamsteering angle and distorted signals at broadside.

in practice via a look-up table of the differential complex radiation patterns between the two states. By checking the radiation pattern of the two states shown in Fig. 17(a), at an angle of 122° for example, only phase calibration is needed since there is a small amplitude difference. However, a more general case can be considered by steering the information beam to angle 46° which has an amplitude difference of almost 10 dB. By correcting the amplitude and phase imbalance, the information beam was steered to 46° as shown in Fig. 20. In Fig. 20, we see that a distorted constellation diagram and eye diagram appear at 0° while standard constellation and eye diagrams are obtained at 46°, demonstrating the ability to steer the information beam.

VII. Conclusion

A new and simple approach to directional modulation using a dynamic antenna was introduced and demonstrated through a $3\lambda/2$ printed dynamic dipole antenna operating at 2.385 GHz. The introduction of a dynamic antenna supports directional modulation in a single antenna element, where prior works have used arrays or multiple signal feeds. The dynamic antenna approach is thus applicable to compact wireless system applications where arrays or the generation of multiple RF input signals is not feasible. Furthermore, our approach can be implemented as a "black box" such that its operation can be transparent to the rest of the wireless system, providing a new form of security at the physical layer that is applicable to both sensing and communications. In addition, the underlying theoretical concept of using dynamic amplitude and phase patterns for directional modulation by a single structure is applicable to other types of antennas beyond that shown in this work, and can even be used in conjunction with other directional modulation designs. Our experimental results demonstrated the ability to maintain low BER in an intended direction (both broadside and steered) while mitigating the ability to demodulate the information at other angles. The gain of the dipole antenna can be further improved by better matching of the switches to the antenna elements, and a more detailed implementation of directional elements can potentially improve overall gain and FBR.

References

[1] Y. Zou, J. Zhu, X. Wang, and L. Hanzo, "A survey on wireless security: Technical challenges, recent advances, and future trends," *Proceedings of the IEEE*, vol. 104, no. 9, pp. 1727–1765, 2016.

[2] C. Miller and C. Valasek, "Securing self-driving cars (one company at a time)," *Black Hat*, 2018.

[3] P. Kapoor, A. Vora, and K.-D. Kang, "Detecting and mitigating spoofing attack against an automotive radar," in *2018 IEEE 88th Vehicular Technology Conference (VTC-Fall)*, 2018, pp. 1–6.

[4] Y.-S. Shiu, S. Y. Chang, H.-C. Wu, S. C.-H. Huang, and H.-H. Chen, "Physical layer security in wireless networks: a tutorial," *IEEE Wireless Communications*, vol. 18, no. 2, pp. 66–74, 2011.

[5] B. Ottersten, "Array processing for wireless communications," in *Proceedings of 8th Workshop on Statistical Signal and Array Processing*, 1996, pp. 466–473.

[6] M. P. Daly and J. T. Bernhard, "Directional modulation technique for phased arrays," *IEEE Transactions on Antennas and Propagation*, vol. 57, no. 9, pp. 2633–2640, 2009.

[7] M. P. Daly and J. T. Bernhard, "Beamsteering in pattern reconfigurable arrays using directional modulation," *IEEE Transactions on Antennas and Propagation*, vol. 58, no. 7, pp. 2259–2265, 2010.

[8] M. P. Daly and J. T. Bernhard, "Directional modulation and coding in arrays," in *2011 IEEE international symposium on antennas and propagation (APSURSI)*. IEEE, 2011, pp. 1984–1987.

[9] Y. Ding and V. F. Fusco, "A vector approach for the analysis and synthesis of directional modulation transmitters," *IEEE Transactions on Antennas and Propagation*, vol. 62, no. 1, pp. 361–370, 2013.

[10] M. P. Daly, E. L. Daly, and J. T. Bernhard, "Demonstration of directional modulation using a phased array," *IEEE Transactions on Antennas and Propagation*, vol. 58, no. 5, pp. 1545–1550, 2010.

[11] A. Babakhani, D. B. Rutledge, and A. Hajimiri, "Transmitter architectures based on near-field direct antenna modulation," *IEEE Journal of Solid-State Circuits*, vol. 43, no. 12, pp. 2674–2692, 2008.

[12] S. M. Ellison, J. M. Merlo, and J. A. Nanzer, "Distributed antenna array dynamics for secure wireless communication," *IEEE Transactions on Antennas and Propagation*, vol. 70, no. 4, pp. 2740–2749, 2022.

[13] A. Narbudowicz, M. J. Ammann, and D. Heberling, "Directional modulation for compact devices," *IEEE Antennas and Wireless Propagation Letters*, vol. 16, pp. 2094–2097, 2017.

[14] J. Parron, E. A. Cabrera-Hernandez, A. Tennant, and P. De Paco, "Multiport compact stacked patch antenna with 360° beam steering for generating dynamic directional modulation," *IEEE Transactions on Antennas and Propagation*, 2020.

[15] N. Valliappan, A. Lozano, and R. W. Heath, "Antenna subset modulation for secure millimeter-wave wireless communication," *IEEE Transactions on communications*, vol. 61, no. 8, pp. 3231–3245, 2013.

[16] Q. Zhu, S. Yang, R. Yao, and Z. Nie, "Directional modulation based on 4-d antenna arrays," *IEEE Transactions on Antennas and Propagation*, vol. 62, no. 2, pp. 621–628, 2013.

[17] Y. Ding and V. Fusco, "A synthesis-free directional modulation transmitter using retrodirective array," *IEEE Journal of Selected Topics in Signal Processing*, vol. 11, no. 2, pp. 428–441, 2016.

[18] A. Abu Arisheh, J. Merlo, and J. A. Nanzer, "Directional modulation using amplitude and phase pattern dynamics of a single antenna," in *2021 USNC-URSI Radio Science Meeting*, 2021.

[19] A. Abu Arisheh, J. Merlo, and J. A. Nanzer, "A dynamic pattern dipole antenna for secure wireless communications," *2022 IEEE International Symposium on Antennas and Propagation and USNC-URSI Radio Science Meeting*.

[20] E. A. Cabrera-Hernández, J. Parrón, and A. Tennant, "Multibeam directional secure transmission with multiport compact antenna," in *2022 16th European Conference on Antennas and Propagation (EuCAP)*. IEEE, 2022, pp. 1–5.

[21] A. Zandamela, N. Marchetti, and A. Narbudowicz, "Directional modulation from a wrist-wearable compact antenna," in *2022 16th European Conference on Antennas and Propagation (EuCAP)*. IEEE, 2022, pp. 1–5.
[22] M. Jamaluddin, M. Rahim, M. A. Aziz, and A. Asrokin, "Microstrip dipole antenna for wlan application," in *2005 1st International Conference on Computers, Communications, & Signal Processing with Special Track on Biomedical Engineering*. IEEE, 2005, pp. 30–33.
[23] M. Jamaluddin, M. Rahim, M. A. Aziz, and A. Asrokin, "Microstrip dipole antenna analysis with different width and length at 2.4 ghz," in *2005 Asia-Pacific Conference on Applied Electromagnetics*. IEEE, 2005, pp. 4–pp.
[24] Y. Yang, Z. Li, S. Wang, X. Chen, J. Wang, and Y. J. Guo, "Miniaturized high-order-mode dipole antennas based on spoof surface plasmon polaritons," *IEEE Antennas and Wireless Propagation Letters*, vol. 17, no. 12, pp. 2409–2413, 2018.
[25] Y. Luo and Z. N. Chen, "Compressed dipoles resonating at higher order modes with enhanced directivity," *IEEE Transactions on Antennas and Propagation*, vol. 65, no. 11, pp. 5697–5701, 2017.

Amer Abu Arisheh (Graduate Student Member, IEEE) received the BS.c. degree in Electrical Engineering from The University of Jordan, Amman, Jordan and his MS.c. degree in Electrical Engineering/Wireless Communications from Jordan University of Science and Technology, Irbid, Jordan. He is currently pursuing the Ph.D. degree in electrical engineering at Michigan State University, East Lansing, MI, USA in 2018. His research interests include dynamic antennas and fundamental electromagnetics.

Jason M. Merlo (Graduate Student Member, IEEE) received the B.S. degree in computer engineering from Michigan State University, East Lansing, MI, USA in 2018, where he is currently pursuing the Ph.D. degree in electrical engineering.

From 2017-2021 he was project manager and electrical systems team lead of the Michigan State University AutoDrive Challenge team. His current research interests include distributed radar and wireless system synchronization, interferometric arrays, synthetic aperture radar, joint radar-communications, and automotive/automated vehicle radar applications.

Jeffrey A. Nanzer (S'02–M'08–SM'14) received the B.S. degrees in electrical engineering and in computer engineering from Michigan State University, East Lansing, MI, USA, in 2003, and the M.S. and Ph.D. degrees in electrical engineering from The University of Texas at Austin, Austin, TX, USA, in 2005 and 2008, respectively.

From 2008 to 2009 he was with the University of Texas Applied Research Laboratories in Austin, Texas as a Post-Doctoral Fellow designing electrically small HF antennas and communications systems. From 2009 to 2016 he was with the Johns Hopkins University Applied Physics Laboratory where he created and led the Advanced Microwave and Millimeter-Wave Technology Section. In 2016 he joined the Department of Electrical and Computer Engineering at Michigan State University where he held the Dennis P. Nyquist Assistant Professorship from 2016 through 2021. He is currently an Associate Professor. He directs the Electromagnetics Laboratory, which consists of the Antenna Laboratory, the Radar Laboratory, and the Wireless Laboratory. He has published more than 200 refereed journal and conference papers, two book chapters, and the book Microwave and Millimeter-Wave Remote Sensing for Security Applications (Artech House, 2012). His research interests are in the areas of distributed phased arrays, dynamic antenna arrays, millimeter-wave imaging, remote sensing, millimeter-wave photonics, and electromagnetics.

Dr. Nanzer is a Distinguished Microwave Lecturer for the IEEE Microwave Theory and Techniques Society (Tatsuo Itoh Class of 2022-2024). He was a Guest Editor of the Special Issue on Special Issue on Radar and Microwave Sensor Systems in the IEEE Microwave and Wireless Components Letters in 2022. He is a member of the IEEE Antennas and Propagation Society Education Committee and the USNC/URSI Commission B, was a founding member and the First Treasurer of the IEEE APS/MTT-S Central Texas Chapter, served as the Vice Chair for the IEEE Antenna Standards Committee from 2013 to 2015, and served as the Chair of the Microwave Systems Technical Committee (MTT-16), IEEE Microwave Theory and Techniques Society from 2016 to 2018. He was a recipient of the Google Research Scholar Award in 2022 and 2023, the IEEE MTT-S Outstanding Young Engineer Award in 2019, the DARPA Director's Fellowship in 2019, the National Science Foundation (NSF) CAREER Award in 2018, the DARPA Young Faculty Award in 2017, and the JHU/APL Outstanding Professional Book Award in 2012. He is currently an Associate Editor of the IEEE TRANSACTIONS ON ANTENNAS AND PROPAGATION.